An In Vitro Perfusion System to Enhance Outflow Studies in Mouse Eyes

Krishnakumar Kizhatil,[1] Arthur Chlebowski,[1] Nicholas G. Tolman,[1] Nelson F. Freeburg,[1] Margaret M. Ryan,[1] Nicholas N. Shaw,[1] Alexander D. M. Kokini,[1] Jeffrey K. Marchant,[2] and Simon W. M. John[1,3]

[1]The Howard Hughes Medical Institute, and The Jackson Laboratory, Bar Harbor, Maine, United States
[2]Department of Integrative Physiology and Pathobiology, Tufts University School of Medicine, Boston, Massachusetts, United States
[3]Department of Ophthalmology and Sackler School of Graduate Biomedical Sciences, Tufts University of Medicine, Boston, Massachusetts, United States

Correspondence: Simon W.M. John, The Howard Hughes Medical Institute, The Jackson Laboratory, 600 Main Street, Bar Harbor, ME 04609, USA; simon.john@jax.org.

Submitted: March 2, 2016
Accepted: August 19, 2016

Citation: Kizhatil K, Chlebowski A, Tolman NG, et al. An in vitro perfusion system to enhance outflow studies in mouse eyes. *Invest Ophthalmol Vis Sci*. 2016;57:5207–5215. DOI: 10.1167/iovs.16-19481

Purpose. The molecular mechanisms controlling aqueous humor (AQH) outflow and IOP need much further definition. The mouse is a powerful system for characterizing the mechanistic basis of AQH outflow. To enhance outflow studies in mice, we developed a perfusion system that is based on human anterior chamber perfusion culture systems. Our mouse system permits previously impractical experiments.

Methods. We engineered a computer-controlled, pump-based perfusion system with a platform for mounting whole dissected mouse eyes (minus lens and iris, ~45% of drainage tissue is perfused). We tested the system's ability to monitor outflow and tested the effects of the outflow-elevating drug, Y27632, a rho-associated protein kinase (ROCK) inhibitor. Finally, we tested the system's ability to detect genetically determined decreases in outflow by determining if deficiency of the candidate genes *Nos3* and *Cav1* alter outflow.

Results. Using our system, the outflow facility (*C*) of C57BL/6J mouse eyes was found to range between 7.7 and 10.4 nl/minutes/mm Hg (corrected for whole eye). Our system readily detected a 74.4% Y27632-induced increase in *C*. The NOS3 inhibitor L-N^G-nitroarginine methyl ester (L-NAME) and a *Nos3* null mutation reduced *C* by 28.3% and 35.8%, respectively. Similarly, in *Cav1* null eyes *C* was reduced by 47.8%.

Conclusions. We engineered a unique perfusion system that can accurately measure changes in *C*. We then used the system to show that NOS3 and CAV1 are key components of mechanism(s) controlling outflow.

Keywords: conventional outflow, mouse model, perfusion system, endothelial Nitric oxide synthase, caveolin

Intraocular pressure elevation is a major causal risk factor for glaucoma.[1] The resistance to aqueous humor (AQH) outflow is a key determinant of IOP.[1] The major site(s) of resistance to AQH drainage have not been determined precisely but are thought to be within or close to the inner wall of the Schlemm's canal (SC). Along with the trabecular meshwork (TM), Schlemm's canal is a critical structure in the pressure-dependent AQH drainage pathway.[1] Increased resistance to drainage and pathologic IOP elevation are thought to result from direct or indirect insults that cause dysfunction of SC/TM cells. Much remains to be learned about the genes and molecular pathways that contribute to normal outflow, and to the etiology of increased outflow resistance underlying high IOP. The molecular mechanisms mediating outflow and the precise route(s) of AQH flow across the SC inner wall need further clarification. Paracellular and transcellular routes of AQH outflow have been proposed based on observation of pores, between or within cells, in fixed or frozen tissue.[2] The route of flow has not been visualized in real-time in living tissue.

Mouse outflow physiology is remarkably similar to that of humans in terms of conventional (pressure-dependent) outflow[3–6] with similarities in IOP values,[7] SC and TM anatomy,[8,9] and lack of "washout" (defined as the increase in outflow that occurs during prolonged ocular perfusion as happens in other nonhuman species).[10] This makes the mouse a powerful model for determining the mechanistic basis of outflow.[6,11–16] The mouse's relatively small size combined with the wealth of genetic and physiologic tools available, and the relatively low costs of maintenance make the mouse an ideal system for large-scale screens for drugs affecting outflow.

A key parameter in the study of outflow physiology is the outflow facility (*C*).[4,10,17] Currently, mouse facility is measured by cannulation either in vivo or in enucleated eyes.[4,10,17] Measurement of C by cannulation is subject to several physical factors (hydration and temperature) that must be carefully monitored.[18] In addition, microleaks around the needle at the point of entry are a concern. In live mice, eyeball movements and twitching can cause the needle to come out of the eye, resulting in failed experiments. The bulky nature of the experimental setup precludes studying pressure-dependent flow in real time by live imaging under high-resolution microscopes. There is a need for a versatile system where

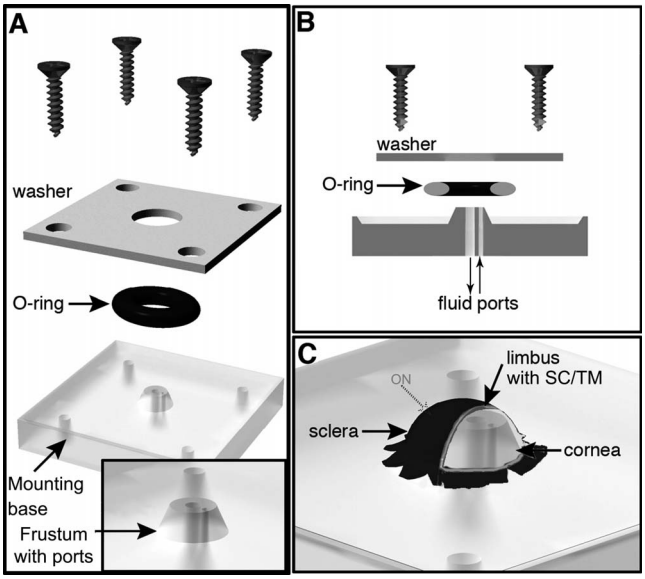

Figure 1. Schematic of the perfusion apparatus with a mounted eye. (**A**) The device consists of a base with central frustum onto which the eye is mounted. The frustum has two fluid ports (see [**B**]) for addition and removal of fluids. The eye is held in place using an O-ring that seals the eye against the frustum. A mounting washer and 4 screws hold the O-ring in place creating a tight seal. (**B**) A cross-sectional view of the system. (**C**) The mounted eye is oriented so that approximately 45% of the limbal tissue, including the drainage structures, is clear of where the O-ring clamps the tissue. Approximate position of the optic nerve (ON) stub is indicated. Images not to scale.

one can measure *C*, culture eyes, and perform live imaging of the intact outflow pathway.

One attractive solution is the use of an in vitro outflow perfusion apparatus. This type of apparatus has been used to measure outflow in eyes of humans and other species, and to organ culture eyes.[19–21] The anterior portion of the eye is dissected, mounted, and sealed on the perfusion apparatus, which has inlet and outlets to flush/perfuse fluids into the eye. To measure outflow, fluid is perfused in while maintaining different pressures. The ability to quickly and gently flush fluids (containing tracers, drugs, viruses) into the anterior chamber gives this method a distinct advantage over cannulation where this typically is impractical. Eyes also can be maintained in culture by using the appropriate media. As the ocular wall is thin in mice, a mouse anterior chamber perfusion culture style system ultimately may allow real-time imaging at high resolution. Due to the various challenges posed by the small size of the mouse eyes and the delicate nature of the tissue, this type of system has not existed for mouse eyes. A mouse system would advance the state of the art by allowing outflow measurements, long-term organ culture, and live imaging in a powerful experimental animal. We report the development of a perfusion system for mouse eyes that allows accurate measurement of outflow and can be used potentially for relatively long-term organ culture and live imaging.

Materials and Methods

Animals

All experiments were performed in compliance with the Association for Research in Vision and Ophthalmology (ARVO) Statement for the Use of Animals in Ophthalmic and Vision Research and the approval of The Jackson Laboratory Institutional Animal Care and Use Committee (IACUC). All mice (3–5 months old and matched sexes) were obtained through The Jackson Laboratory. The mice were kept on a standard 14-hour light/10-hour dark cycle with food and water available ad libitum. The mouse strains used are shown in the Supplementary Methods.

Perfusion Apparatus

A mouse eye perfusion apparatus was engineered based on a human anterior segment perfusion apparatus (Fig. 1, Supplementary Fig. S1).[19,20] Our apparatus, milled from Lexan, consisted of a base with a conical frustum for mounting eyes (Fig. 1, Supplementary Fig. S1).The top of the frustum had a diameter of 2.7 mm and the base 3.4 mm. We built our first system based on the human apparatus, which had a large footprint (Supplementary Fig. S1). We then redesigned that base to reduce the footprint and for ease of manufacture (Fig. 1). Most importantly the frustum design and performance were identical in both devices (Supplementary Fig. S2). The frustum had fluid inlet and outlet channels running from the base to the top. In our newer systems, 26-gauge needles (Becton Dickinson, Franklin Lakes, NJ, USA) were inserted into the inlet and outlet channels at the frustum base and bent gently to a curve. The needles were sealed into the inlet and outlet channels (henceforth ports) using epoxy glue.

Mounting a Dissected Eye on Perfusion Apparatus

A dissected eye (see Supplementary Methods) was kept moist, and mounted carefully and gently onto the frustum using the opening in the side of the globe. The flaps cut into the sclera allowed the eye to sit on the frustum, and the flaps were lightly glued onto the platform bearing the frustum (using tissue glue) to hold the eye in position. A seal was created between the eye and frustum using an O-ring and washer (Fig. 1). The washer was secured in place by four corner screws that insert into the base. For uniformity, all screws were symmetrically and equally tightened using a torque screwdriver (10 cN.m; Fig. 1). In this configuration the limbus of the eye spans the top of the frustum with sclera on one side and cornea on the other side. Although the retina is removed, the retinal pigment epithelium layer is maintained intact and lines the sclera. The eye was checked for a pressure-tight seal by gently pushing in test perfusate (Dulbecco's PBS [DPBS], balanced salt solution [BSS], or a drug mixture) through the inlet port, after closing the outlet port, using a three-way stopcock to determine if the flaccid eye mounted on the frustum inflated without visible leaks around the O-ring.

The inlet port then was connected to a pressure transducer (DTXPlus TNF-R; Argon Medical Systems, Plano, TX, USA; see Supplementary Methods for details), in series with a perfusate-filled 100 µl Nanofil syringe (Worcester Polytechnic Institute [WPI], Worcester, MA, USA) attached to a UMP3 pump (WPI) controlled by a Micro-4 pump controller (WPI). The transducer was connected to the apparatus with a short length of pressure-resistant tubing. Any air bubbles in the system were removed carefully using the perfusion fluid of choice. The pressure transducer connects to the computer via a digitizer (Measurement Computing, Norton, MA, USA) and with the microprocessor controller we created closed-loop control (WPI; see below). The eye was maintained in a moist state at 37°C by inverting the eye over a well of a heating block filled with water (to a height approximately 1 mm below the eye, see Fig. 2B) during measurement of outflow.

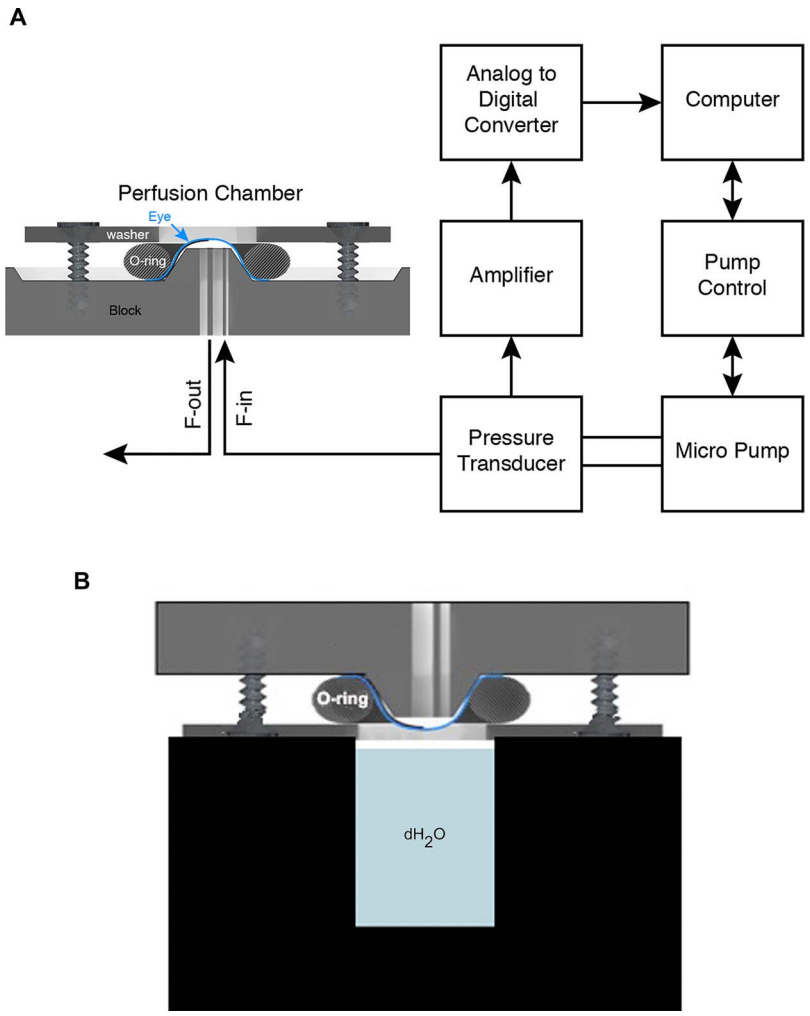

Figure 2. Schematic of system control. (**A**) The eye is sealed onto the perfusion device and fluid (saline, drugs, and tracers) is introduced or drained through the two ports (F-in, F-out). F-out is closed except when flushing. The F-in port is connected to a pressure transducer, which in turn is connected to a micropump. The pressure transducer monitors IOP constantly and supplies this information to the computer, which control the pump controller and pump. The control algorithm maintains pressures at the desired values and durations according to the preset experimental plan. (**B**) Schematic showing a mounted eye in a humidifying chamber that is maintained at 37°C (not to scale).

Monitoring and Control System

While measuring outflow, fluid was perfused at a controlled rate to maintain the eye at a specific pressure. The perfusion rate was monitored and controlled by an in-house computer program (LabVIEW; National Instruments, Austin, TX, USA) using a bang-bang control algorithm. The steady state error of the system was ±0.5 mm Hg. Once started, the program continuously monitored and recorded information from the pressure transducer and flow rate information from the syringe pump microprocessor controller. If pressure fell by a small fraction of 1 mm Hg below the set level, the program triggered the syringe pump to perfuse fluid into the eye via the microprocessor controller. As soon as the pressure increased to a fraction of 1 mm Hg above the set point the pump turned off. As the pump delivered fluid in increments of 0.67 nL/step, flow continued after the pump was shut off, explaining the oscillatory nature of the flow rate plot. The software was designed to set different experimental pressure levels in a stepwise manner (up to six pressure values can be input). The user set the "rise" time to reach a set pressure, the "equilibration" time for the eye to adjust to that pressure, and a "record" time to measure flow rate required to maintain the pressure. The rise and equilibration time ensured that we recorded data only after the flow rate oscillations had reached a stable state.

Outflow Measurements

Before outflow measurement on any day, we calibrated the pressure transducer using a mercury manometer. Outflow was measured by obtaining the flow rate required to maintain a series of set pressures. We use two pressure series: Protocol A – 5, 15, 25, 35, 45, and then 15 mm Hg again, and Protocol B – 8, 12, 16, 20, 24, and 12 mm Hg again. In both protocols, rise time was 5 minutes, equilibration time was 5 minutes, and record time was 10 minutes (see Monitoring and control section above). A run was considered successful if the following criteria were met in analysis of the data: (1) Flow rates at each pressure achieved stable oscillation about a mean with oscillations being no more than ±30 nL for 5, 15, and 25 mm Hg pressure set points, and (2) Flow rates were similar at the

Investigative Ophthalmology & Visual Science

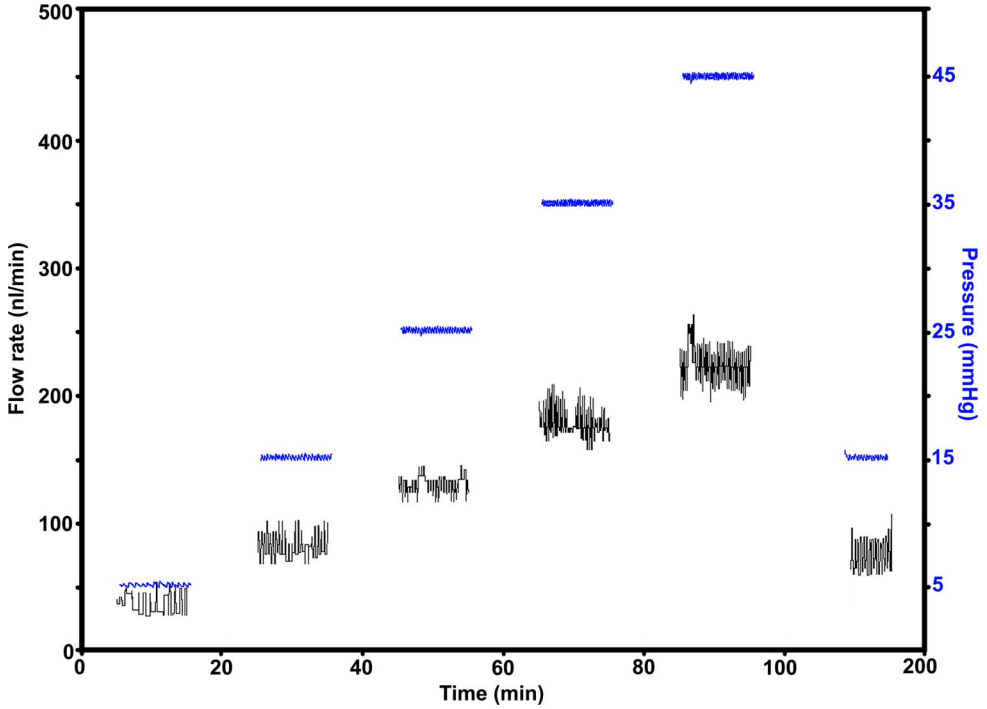

Figure 3. Flow rates and pressure profiles. The plot shows the flow rate and pressure traces recorded during perfusion of a representative eye (Protocol A, see Methods). The axis on the *left* shows flow rate (nL/min) and the one on the *right* pressure (mm Hg). Pressure traces are in *blue*.

first and second 15 mm Hg (Protocol A) or first and second 12 mm Hg (Protocol B). Our success rate was over 90%. If an eye failed at any pressure, all data for that eye were discarded. Drugs were perfused in at 15 mm Hg for 30 minutes followed by 15 minutes at 5 mm Hg before measuring outflow. We used Y27632 at 200 μM and L-N^G-nitroarginine methyl ester (L-NAME) at 100 μM. No eyes were perfused for longer than 2 hours and some eyes were fixed for immunofluorescence or histology (see Supplementary Methods) after outflow measurements were concluded.

Results

The Perfusion System

The system consisted of a perfusion platform with a conical frustum for mounting the eye (Fig. 1, Supplementary Fig. S1) and a micropump fluid perfusion system controlled by a computer (Fig. 2A). We first determined the best way to mount eyes onto the frustum. Due to mouse anatomy, mounting the anterior segment of the eye "cornea up," as with human anterior segments, placed the limbus too close to all clamping mechanisms that we devised. This risked crushing the drainage structures and blocking outflow. Thus, we mounted the eye with the limbus up and spanning the top of the frustum (therefore, ~45% of the limbal circumference was available for perfusion; see Supplementary Methods). This approach provided ample clearance from the O-ring and an orientation that would ultimately facilitate live imaging. To enable this, we developed the dissection scheme that is shown in Supplementary Figures S3 and S4 (see Supplementary Methods). The dissection of the eye is a critical and delicate step that requires attention to detail.

Characterization of the System: System Compliance and Resistance

Before performing any outflow measurements, we tested the system for any inherent resistance and compliance (defined as change in flow rate in response to pressure caused by any elasticity in the system). It is critical to determine these parameters because they can make outflow measurement inaccurate. Upon using a flow rate of 660 μl/min (far larger than the flow observed by an eye) and leaving the inlet port open (no eye secured to system), we observed no increase over atmospheric pressure (0 mm Hg), indicating that the system had no measurable resistance at this flow rate (or under physiologic conditions). System compliance was determined to be 20.65 nL/mm Hg (see Supplementary Methods).

Washout in Mouse Eye

Washout (*C* increase upon prolonged ocular perfusion) is observed in some nonhuman species, including primates but not humans or mice.[10,22–25] The washout rate for mouse eyes using our system was 2.5 ± 1.96% ($n = 6$), in agreement with an earlier study (washout rate = 2.4%)[10] and in contrast to monkey eyes, where the washout rate is 26% to 42%.[24] Thus, we confirmed that mouse eyes, like human eyes,[25] have negligible washout.

Outflow Measurements

We determined *C* in mouse eyes by computing the slope of the flow rate versus pressure plot (Protocols A and B, see Supplementary Methods).[10] An example of recorded pressure and flow rate traces is shown in Figure 3. Importantly, this plot shows that the flow rates at 15 mm Hg at the beginning and end of the perfusion protocol are similar, indicating that the

Investigative Ophthalmology & Visual Science

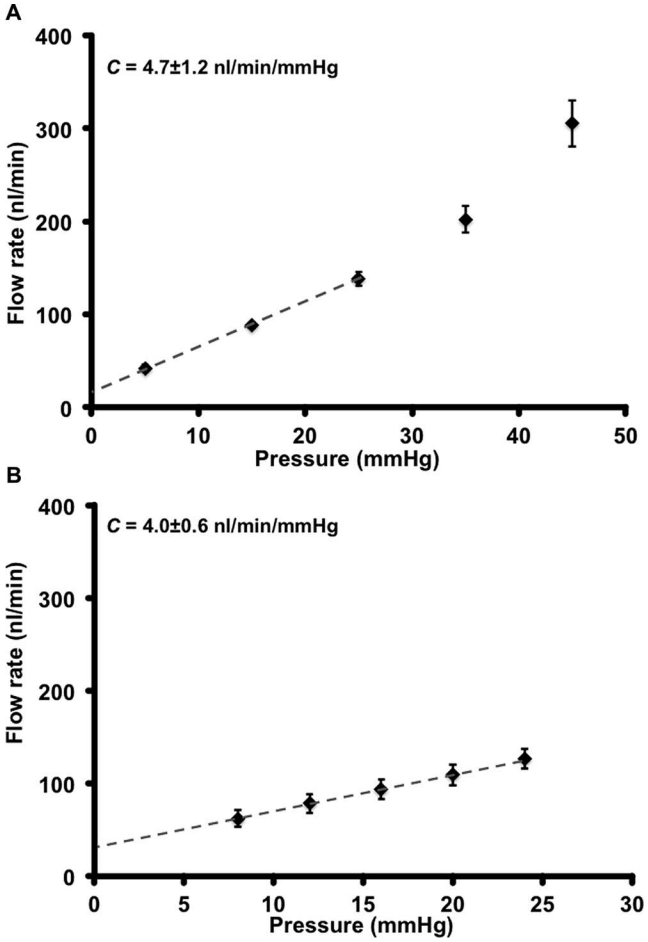

FIGURE 4. Flow rates and facility. (**A**) Eyes ($n = 10$) perfused at 5, 15, 25, 35, and 45 mm Hg (Protocol A). The flow rate to pressure relationship is biphasic: it is linear up to 25 mm Hg (*dashed line*), after which its rate of change increased. The equation of the line for the linear range was $y = 0.0047x + 0.0175$, and the quality of linear fit $R^2 = 0.99946$. The slope of flow rate change with pressure in this linear range is the $C = 4.7 \pm 1.2$ nL/min/mm Hg. When corrected to match whole eyes (as only 45% of drainage tissue is available in mounted eyes) $C = 10.4 \pm 2.64$ nL/min/mm Hg. (**B**) Eyes ($n = 8$) perfused over a narrower pressure range of 8, 12, 16, 20, and 24 mm Hg (Protocol B). The line of fit for the linear part of the plot, $y = 0.004x + 0.03$, $R^2 = 0.9995$, gives a C value of 4.0 ± 0.6 nL/min/mm Hg. When corrected for the whole eye $C = 8 \pm 1.32$ nL/min/mm Hg. C = mean ± SD. SEM is shown for data points in the graph.

drainage tissue is undamaged. Flow rates versus pressure graphs are depicted in Figures 4A (Protocol A, $n = 10$) and 4B (Protocol B, $n = 8$). In these graphs, the plotted curve approximated linearity up to 25 mm Hg and showed an upward deviation after 25 mm Hg (Fig. 4A). The linear nature is clear when outflow is measured using more points within the narrower pressure range of Protocol B. Protocol A was used to understand flow rate changes over a wide range of pressure. We primarily have used Protocol A in this study. Protocol B, with more points in the linear range, will be useful when there is a need for high precision measurement of suspected flow rate changes at low pressures or when changes are subtle.

We obtained C values of 4.7 ± 1.2 nL/min/mm Hg (mean ± SD) using Protocol A and 4.0 ± 0.6 nL/min/mm Hg by Protocol B in eyes of B6 mice. There was no significant difference in C values obtained by either Protocols A or B ($P = 0.095$). The y-intercepts in the flow rate versus pressure plots, often considered a measure of pressure-independent flow,[10] was 17.5 nL/min and 30 nL/min for Protocols A and B, respectively.

The absolute value of facility depends on how much of the outflow pathway is being perfused. In our experiments, approximately 45% of the limbal circumference (see Supplementary Methods) was available for perfusion. Therefore, the measured facility must be increased by a factor of 2.2 to estimate the facility for the entire outflow pathway. Thus, the C values for the whole eye would be 10.34 ± 2.64 nL/min/mm Hg using Protocol A and 8.0 ± 1.32 nL/min/mm Hg using Protocol B.

To determine if the drainage structures are intact after outflow assessment, we used our recently described technique and *Prox1-GFP* eyes[8] to image large swaths of the SC at a subcellular level after outflow measurement (as SC inner wall is the last barrier to drainage). Following Protocol A ($n = 6$, Fig. 5), vascular endothelial (VE)–cadherin staining showed that the cell shape and cell junctions were intact and comparable in control and perfused eyes (Fig. 5B). Retention of green fluorescent protein (GFP) signal in SC after outflow, and lack of intracellular propidium iodide (included in perfusate, data not shown) in limbal tissue, indicated the absence of membrane damage to the drainage structure cells. These results also indicated that the integrity of SC inner wall endothelia was uncompromised at a cellular level. Similarly, conventional sections (see Supplementary Methods) showed that a perfused eye (protocol A) had an open SC and intact TM that were comparable to those in a control eye with intact iris (Fig. 5C). Using a fluorescent 3-kDa Dextran tracer, we also showed that flow was restricted to the drainage structures, SC and TM. No tracer fluorescence was observed in the sclera or RPE (Supplementary Fig. S5).

Inhibition of Rho-Associated Protein Kinase (ROCK) Increases Outflow

We next determined if perturbation of outflow at a molecular level can be detected using our perfusion device. We first tested the effect of the ROCK inhibitor, Y-27632 (see Supplementary Methods for details), on C. Y-27632 is well established to increase outflow in other species.[26–28] We observed a 74.4% increase in C in eyes treated with Y-27632 ($n = 10$, t-test $P = 0.003$; Fig. 6). Thus, as expected, ROCK inhibition increased C. This experiment validated the use of our system to measure changes in C.

Nos3 and *Cav1* Are Required for Proper Outflow

Nos3 (endothelial nitric oxide synthase, eNOS) and *Cav1*[29,30] are genes implicated in glaucoma. It is unclear how these genes impact the disease. Hence, we determined if these genes were required for normal outflow. We first disrupted *Nos3* function by inhibition using the inhibitor L-NAME; see Supplementary Methods for details) as well as through genetic mutation. Treatment with L-NAME caused a reduction in C by 28.3% from control ($n = 7$ eyes; t-test, $P = 0.025$; Fig. 7A). In *Nos3* null mutant eyes C was reduced by 35.8% compared to control ($n = 7$ eyes; t-test, $P = 0.008$; Fig. 7B). Next, we performed outflow measurements on *Cav1* null (*Cav1*$^{-/-}$) eyes ($n = 9$ eyes; Fig. 8). In *Cav1*$^{-/-}$ eyes, C was reduced by 47.8% compared to control (t-test, $P = 0.02$). We detected this reduction in two independent experiments on a B6 strain background and once on a mixed strain background (not shown). These results indicated that NOS3 and CAV1 function are required for normal outflow.

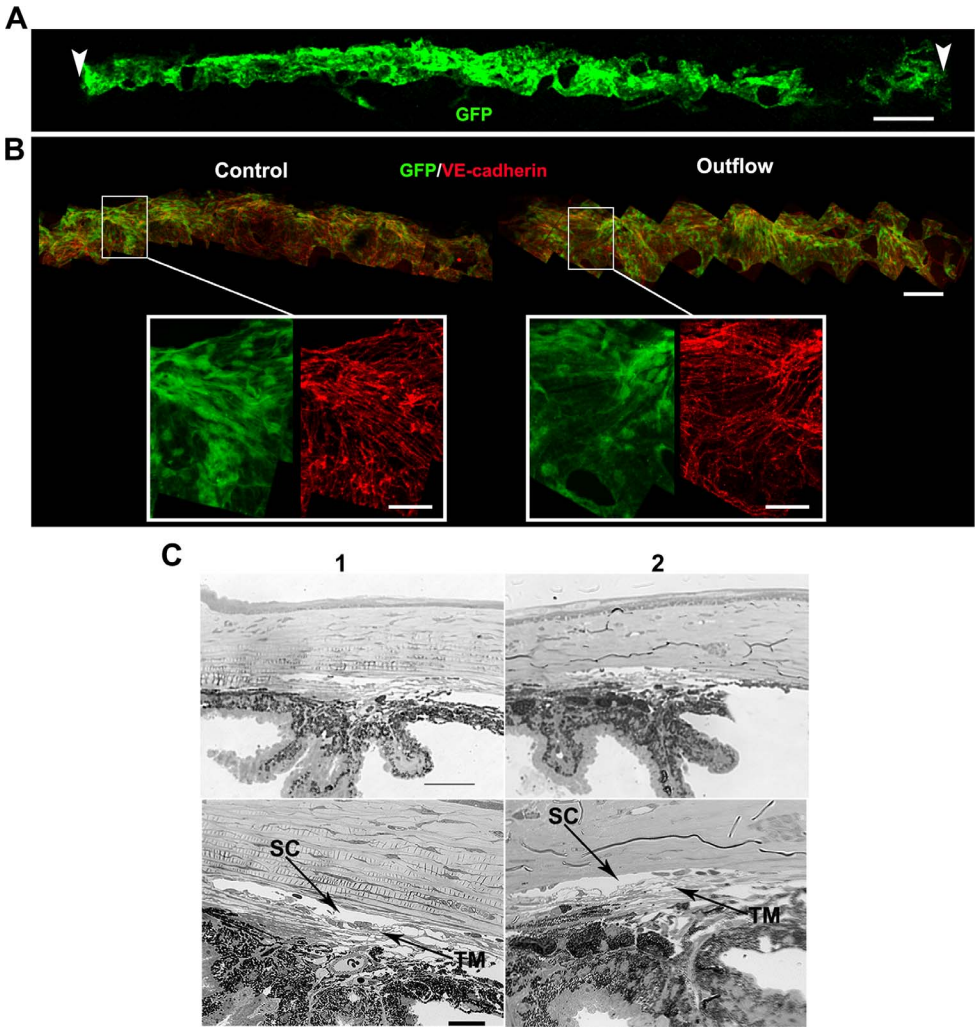

Figure 5. The drainage structures remain intact during mounting and perfusion. (**A**) Whole mount of a *Prox1-GFP* eye after an outflow experiment, showing the entire extent of the limbus and SC (*green*) subjected to flow. Schlemm's canal over this entire length has a normal healthy morphology. Vascular endothelial–cadherin staining (not shown) was present in area low in Prox1-GFP at the right. *Arrowheads* indicate points where the O-ring contacted the limbus when the eye was mounted on the frustum. Typically approximately 45% of the limbus is subjected to flow (see Supplementary Methods). (**B**) Higher magnification images of a freshly dissected control eye and an eye after outflow. The general morphology (GFP, *green*) and cellular junctions (VE-cadherin, *red*) of SC are indistinguishable between these eyes. This indicates that the inner wall SC endothelium is intact. The GFP level in eyes subjected to outflow is always within the range of variability in unperfused control *Prox1-GFP* eyes. Retention of GFP signal after outflow is a good indicator that SC cells are healthy. (It is well established that compromised cell membrane integrity results in leakage of cytoplasmic GFP and reduction in green fluorescence.) $n = 6$ eyes each for control and outflow cohorts. *Scales bars*: (**A**) 300 μm; (**B**) top 100 μm; insets 30 μm. (**C**) Plastic sections of a control (*1*) and perfused (*2*) eye showing the drainage structures. $n = 3$ eyes each for control and outflow cohorts. Images at lower magnification show the angle in the context of the iris and cornea (*top*). Higher magnification images (*bottom*) allow for visualization of the open SC and TM. *Scale bars*: Top, 50 μm; Bottom, 20 μm.

Discussion

We described a new way to study the molecular mechanisms controlling outflow. Using a newly engineered in vitro perfusion system, we first established a mechanistic role for the kinase activity of ROCK in mouse conventional outflow. We also showed that NOS3 and CAV1 function, both previously implicated in glaucoma, is necessary for normal outflow. These studies demonstrated the use of our system for identifying molecules and/or pathways controlling outflow.

Conventional facility measured using our system was in the range described for mouse eyes.[18,31] Several other investigators have described the nonlinearity of the flow rate–pressure plot above 25 mm Hg.[10,18] Recently, it has been determined that anterior chamber deepening with increasing pressure (over 25 mm Hg) in enucleated mouse eyes results in traction on the TM, thus increasing C.[18] Our mounted eyes do not have an intact iris and AC, but similar nonlinearity was observed. Although the mechanism explaining this is not clear, increasing traction on the mounted tissue may itself allow nonlinear increases in outflow with increasing pressure. A recent publication, using closely spaced pressure points and sophisticated data analysis, supports nonlinear changes in outflow with changing pressure.[31]

A recent report suggested that insufficient hydration results in a positive y-intercept and that hydrating enucleated eyes by immersion eliminated this positive y-intercept, actually rendering it negative.[18] During our experiments, we had maintained

Investigative Ophthalmology & Visual Science

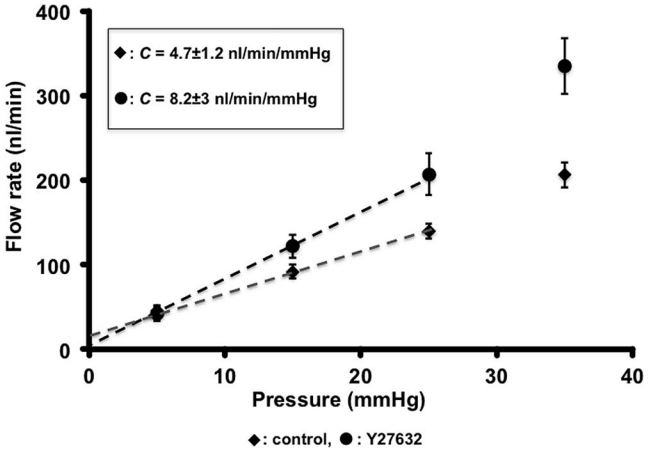

FIGURE 6. Rho-associated protein kinase inhibitor Y27632 increases outflow in mouse eyes. Eyes treated with Y27632 were perfused with 200 μM drug in BSS for 30 minutes at 15 mm Hg, followed by a 15 minutes of perfusion at 5 mm Hg before measuring outflow (Protocol A). Control eyes were treated identically except for the absence of drug. The lines of fit for the linear part of the plots are: Control, $y = 0.0047x + 0.0175$, $R^2 = 0.99946$; Y27632, $y = 0.0082x + 0.0003$, $R^2 = 0.9996$. *C* was different between groups: control, $C = 4.7 \pm 1.2$ nL/min/mm Hg (whole eye $C = 10.4 \pm 2.64$ nL/min/mm Hg); Y27632, $C = 8.2 \pm 3$ nL/min/mm Hg (whole eye $C = 18.04 \pm 6.6$ nL/min/mm Hg). *C* = mean ± SD. SEM is shown for data points in the graph.

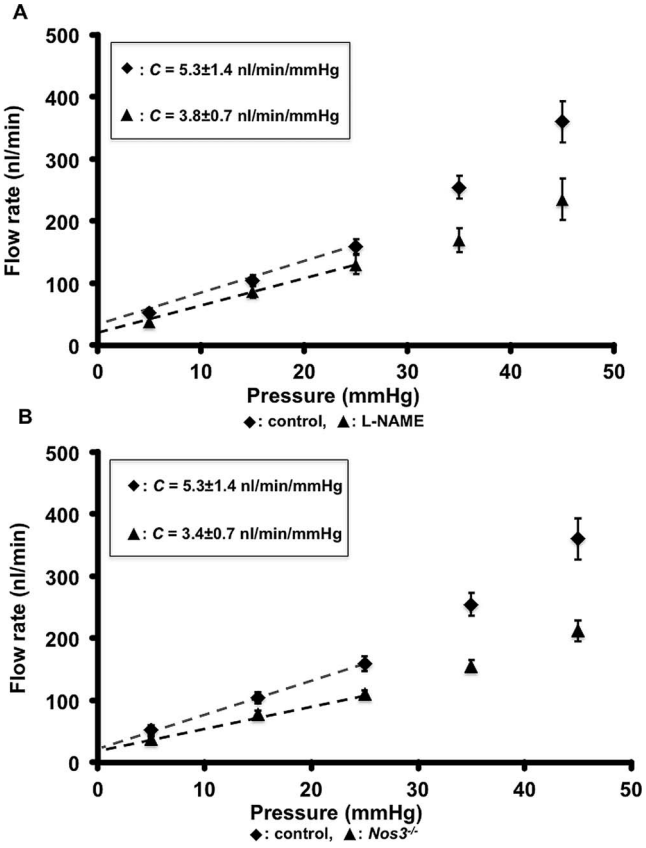

FIGURE 7. Pressure-dependent increases in outflow require NOS3 activity. The requirement of NOS3 activity was tested using *Nos3* mutant or L-NAME–treated wild-type eyes. (**A**) Flow-rate versus pressure graph obtained from L-NAME–treated and control eyes. (**B**) Flow-rate versus pressure graph obtained from $Nos3^{-/-}$ and control eyes. *Black diamonds* represent control eyes and *black triangles* either L-NAME–treated eyes or $Nos3^{-/-}$ eyes. The equations representing the trendline for the linear part of the curve (in [**A**] and [**B**]) were: Control, $y = 0.0053x + 0.0254$, $R^2 = 0.9997$; L-NAME, $y = 0.0038x + 0.0382$, $R^2 = 0.99971$; and $Nos3^{-/-}$ $y = 0.0034x + 0.0211$, $R^2 = 0.9976$. *C* was different between groups: Control, $C = 5.3 \pm 1.4$ nL/min/mm Hg (whole eye $C = 11.6 \pm 3.08$ nL/min/mm Hg); L-NAME, $C = 3.8 \pm 0.7$ nL/min/mm Hg (whole eye $C = 8.36 \pm 1.54$ nL/min/mm Hg); $Nos3^{-/-}$, $C = 3.4 \pm 0.6$ nL/min/mm Hg (whole eye $C = 7.48 \pm 1.32$ nL/min/mm Hg). *C* = mean ± SD. SEM is shown for data points in the graph.

the mounted eyes in a humid environment (measured to be 100% humidity) to prevent evaporation. Nevertheless, our positive intercepts suggested that the humidity measurements might not have been accurate, allowing some evaporation. Thus, in response to this recent report, we performed our perfusion protocol after submerging eyes in PBS at 37°C. The submersion changed the *y*-intercept to −18.5 μl/min, indicating that evaporation from the surface of the eye may be occurring in our humid environment. Importantly, the *C* value obtained when submerging the eyes was $C = 5.065 \pm 1.1$ nL/min/mm Hg. This value is not significantly different from that obtained when eyes were maintained in a humid atmosphere (4.7 ± 1.2 nL/min/mm Hg; $P = 0.49$). This suggested that our original approach of maintaining the eye in the humid atmosphere did not affect measurement of *C*. Importantly and during peer review of the current study, another study found no flow at 0 mm Hg and suggested that negative intercepts are an artifact resulting from linear fitting of data.[31] This study sampled flow at nine pressures over the 5 to 20 mm Hg range. This dense sampling allowed power-fitting with a *y*-intercept of zero at 0 mm Hg. Such dense sampling can be tested with our perfusion system and could improve accuracy in future experiments.

To our knowledge, this is the first report that inhibiting ROCK activity increases conventional outflow in mouse eyes, as it does in other species, including human eyes.[26–28] Our data suggested that the previous report of Y27632 reducing IOP in mice[32] results from increased outflow. Rho-associated protein kinase has been implicated in a mechanosensing role in SC cells by controlling cell stiffness.[33]

Our data, along with a recent report by Lei et al.,[12] showed that NOS3 function is required for conventional outflow regulation. This is supported by additional studies where overexpression of human *Nos3* in mouse eyes resulted in increased outflow and L-NAME reduced outflow.[5,13] On a mechanistic level, biomechanical strain on SC cells triggers activation/expression of NOS3 function[34] to elevate nitric oxide (NO) levels. Increased NO levels increases outflow.[5,33]

Cav1 has been implicated in glaucoma.[30] Given the ubiquitous expression of CAV1, it could be important for IOP, function of retinal ganglion cells, and cells in the optic nerve head. Our data indicated that CAV1 is at least required for conventional drainage and will impact IOP. Given that we used a mutant mouse where *Cav1* is globally deleted, we will in the future perform cell type–specific inhibition to identify the critical cell type that controls outflow through *Cav1* function.

The protein CAV1 has been implicated in mechanotransduction[35] and regulation of *Nos3* activity.[36] Loss of either function (not mutually exclusive) would prevent translation of pressure-dependent strain on SC/TM cells into signals required for outflow.

In summary, we have successfully developed a new perfusion system to study molecular mechanisms controlling outflow. We described a new role for CAV1 in outflow physiology and provide more evidence for central roles for

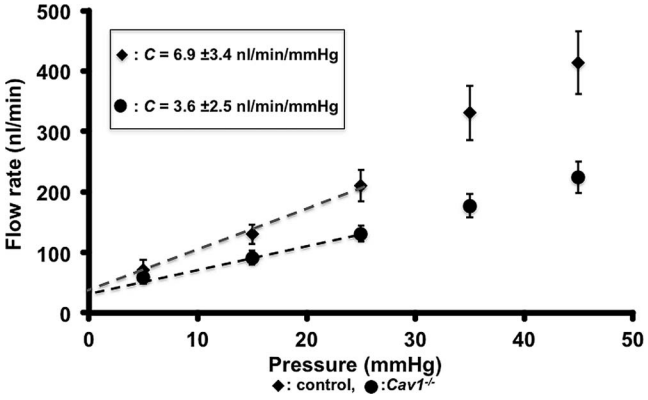

Figure 8. Loss of CAV1 decreases pressure-dependent outflow in mouse eyes. Flow-rate versus pressure graph showing a comparison of flow rates in control and *Cav1*$^{-/-}$ eyes. The equations representing the trend line for the linear part of the curve were: Control, $y = 0.007x + 0.0326$, $R^2 = 0.99322$, *black circles*; *Cav1*$^{-/-}$, $y = 0.0036x + 0.039$, $R^2 = 0.99322$, *black diamond*. SEM is shown for data points in the graph. The computed *C* values were: control, $C = 6.9 \pm 3.4$ nL/min/mm Hg (whole eye $C = 15.18 \pm 4.4$ nL/min/mm Hg), and $C = 3.6 \pm 2.5$ nL/min/mm Hg (whole eye $C = 7.92 \pm 5.5$ nL/min/mm Hg). C = mean ± SD. SEM is shown for data points in the graph.

NOS3 and ROCK in outflow regulation. With its potential for organ culture, our system is expected to allow development of longitudinal physiologic studies and live imaging.

Acknowledgments

The authors thank Teresa Borras, PhD, Department of Ophthalmology, University of North Carolina, for generously sharing the designs of a human perfusion apparatus, and Dave Davis of the Jackson Laboratory for his help in development and fabrication of the device.

Supported by National Institutes of Health (NIH; Bethesda, MD, USA) Grant EY11721. SWMJ is an investigator of HHMI.

Disclosure: **K. Kizhatil**, None; **A. Chlebowski**, None; **N.G. Tolman**, None; **N.F. Freeburg**, None; **M.M. Ryan**, None; **N.N. Shaw**, None; **A.D.M. Kokini**, None; **J.K. Marchant**, None; **S.W.M. John**, None

References

1. Overby DR, Stamer WD, Johnson M. The changing paradigm of outflow resistance generation: towards synergistic models of the JCT and inner wall endothelium. *Exp Eye Res*. 2009;88:656–670.
2. Tamm ER. The trabecular meshwork outflow pathways: structural and functional aspects. *Exp Eye Res*. 2009;88:648–655.
3. Aihara M, Lindsey JD, Weinreb RN. Reduction of intraocular pressure in mouse eyes treated with latanoprost. *Invest Ophthalmol Vis Sci*. 2002;43:146–150.
4. Millar JC, Clark AF, Pang IH. Assessment of aqueous humor dynamics in the mouse by a novel method of constant-flow infusion. *Invest Ophthalmol Vis Sci*. 2011;52:685–694.
5. Stamer WD, Lei Y, Boussommier-Calleja A, Overby DR, Ethier CR. eNOS a pressure-dependent regulator of intraocular pressure. *Invest Ophthalmol Vis Sci*. 2011;52:9438–9444.
6. Nair KS, Hmani-Aifa M, Ali Z, et al. Alteration of the serine protease PRSS56 causes angle-closure glaucoma in mice and posterior microphthalmia in humans and mice. *Nat Genet*. 2011;43:579–584.
7. Savinova OV, Sugiyama F, Martin JE, et al. Intraocular pressure in genetically distinct mice: an update and strain survey. *BMC Genet*. 2011;2:12.
8. Kizhatil K, Ryan M, Marchant JK, Henrich S, John SW. Schlemm's canal is a unique vessel with a combination of blood vascular and lymphatic phenotypes that forms by a novel developmental process. *PLoS Biol*. 2014;12:e1001912.
9. Overby DR, Bertrand J, Schicht M, Paulsen F, Stamer WD, Lütjen-Drecoll E. The structure of the trabecular meshwork, its connections to the ciliary muscle, and the effect of pilocarpine on outflow facility in mice. *Invest Ophthalmol Vis Sci*. 2014;55:3727–3736.
10. Lei Y, Overby DR, Boussommier-Calleja A, Stamer WD, Ethier CR. Outflow physiology of the mouse eye: pressure dependence and washout. *Invest Ophthalmol Vis Sci*. 2011;52:1865–1871.
11. Johnson M, McLaren JW, Overby DR. Unconventional aqueous humor outflow: a review [published online ahead of print February 2 2016]. *Exp Eye Res*.
12. Lei Y, Zhang X, Song M, Wu J, Sun X. Aqueous humor outflow physiology in NOS3 knockout mice. *Invest Ophthalmol Vis Sci*. 2015;56:4891–4898.
13. Chang JYH, Stamer WD, Bertrand J, et al. Role of nitric oxide in murine conventional outflow physiology. *Am J Physiol Cell Physiol*. 2015;309:C205–214.
14. Sano K, Katsuta O, Shirae S, et al. Flt1 and Flk1 mediate regulation of intraocular pressure and their double heterozygosity causes the buphthalmia in mice. *Biochemical Biophys Res Commun*. 2012;420:422–427.
15. Fujikawa K, Iwata T, Inoue K, et al. VAV2 and VAV3 as candidate disease genes for spontaneous glaucoma in mice and humans. *PLoS One*. 2010;5:e9050.
16. John SWM. Mechanistic insights to Glaucoma provided by experimental genetics: the Cogan Lecture. *Invest Ophthalmol Vis Sci*. 2005;46:2650–2661.
17. Aihara M, Lindsey JD, Weinreb RN. Aqueous humor dynamics in mice. *Invest Ophthalmol Vis Sci*. 2003;44:5168–5173.
18. Boussommier-Calleja A, Li G, Wilson A, et al. Physical factors affecting outflow facility measurements in mice. *Invest Ophthalmol Vis Sci*. 2015;56:8331–8339.
19. Johnson DH, Tschumper RC. Human trabecular meshwork organ culture. A new method. *Invest Ophthalmol Vis Sci*. 1987;28:945–953.
20. Comes N, Borras T. Individual molecular response to elevated intraocular pressure in perfused postmortem human eyes. *Physiol Genom*. 2009;38:205–225.
21. Rao PV, Deng PF, Kumar J, Epstein DL. Modulation of aqueous humor outflow facility by the Rho kinase-specific inhibitor Y-27632. *Invest Ophthalmol Vis Sci*. 2001;42:1029–1037.
22. Johnson M, Chen A, Epstein DL, Kamm RD. The pressure and volume dependence of the rate of wash-out in the bovine eye. *Curr Eye Res*. 1991;10:373–375.
23. Sit AJ, Gong H, Ritter N, Freddo TF, Kamm R, Johnson M. The role of soluble proteins in generating aqueous outflow resistance in the bovine and human eye. *Exp Eye Res*. 1997;64:813–821.
24. Scott PA, Overby DR, Freddo TF, Gong H. Comparative studies between species that do and do not exhibit the washout effect. *Exp Eye Res*. 2007;84:435–443.
25. Erickson-Lamy K, Schroeder AM, Bassett-Chu S, Epstein DL. Absence of time-dependent facility increase ("washout") in the perfused enucleated human eye. *Invest Ophthalmol Vis Sci*. 1990;31:2384–2388.
26. Honjo M, Tanihara H, Inatani M, et al. Effects of rho-associated protein kinase inhibitor Y-27632 on intraocular pressure and outflow facility. *Invest Ophthalmol Vis Sci*. 2001;42:137–144.

27. Yang CY, Liu Y, Lu Z, Ren R, Gong H. Effects of Y27632 on aqueous humor outflow facility with changes in hydrodynamic pattern and morphology in human eyes. *Invest Ophthalmol Vis Sci*. 2013;54:5859–5870.
28. Kameda T, Inoue T, Inatani M, et al. The effect of Rho-associated protein kinase inhibitor on monkey Schlemm's canal endothelial cells. *Invest Ophthalmol Vis Sci*. 2012;53:3092–3103.
29. Kang JH, Wiggs JL, Rosner BA, et al. Endothelial nitric oxide synthase gene variants and primary open-angle glaucoma: interactions with sex and postmenopausal hormone use. *Invest Ophthalmol Vis Sci*. 2010;51:971–979.
30. Thorleifsson G, Bragi Walters G, Weitt AW, et al. Common variants near CAV1 and CAV2 are associated with primary open-angle glaucoma. *Nat Genet*. 2010;42:906–909.
31. Sherwood JM, Reina-Torres E, Bertrand JA, Rowe B, Overby DR. Measurement of outflow facility using iPerfusion. *PLoS One*. 2016;11:e0150694.
32. Whitloc NA, Harrison B, Mixon T, et al. Decreased intraocular pressure in mice following either pharmacological or genetic inhibition of ROCK. *J Ocul Pharmacol Ther*. 2009;25:187–194.
33. Stamer WD, Braakman ST, Zhou EH, et al. Biomechanics of Schlemm's canal endothelium and intraocular pressure reduction. *Prog Retin Eye Res*. 2015;44:86–98.
34. Jessop HL, Suswillo RF, Rawlingson SC, et al. Osteoblast-like cells from estrogen receptor alpha knockout mice have deficient responses to mechanical strain. *J Bone Miner Res*. 2004;19:938–946.
35. Sinha B, Küster D, Ruez R, et al. Cells respond to mechanical stress by rapid disassembly of caveolae. *Cell*. 2011;144:402–413.
36. Wunderlich C, Schober K, Schmeisser A, et al. The adverse cardiopulmonary phenotype of caveolin-1 deficient mice is mediated by a dysfunctional endothelium. *J Mol Cell Cardiol*. 2008;44:938–947.

Investigative Ophthalmology & Visual Science